Scientific Research Publishing

Open Journal of Geology, 2024, 14, 855-879
https://www.scirp.org/journal/ojg
ISSN Online: 2161-7589
ISSN Print: 2161-7570

Structural Pattern Related to Gold Mineralization in the Essakane Area (Northern Burkina Faso, West African Craton)

Marc Desire Valea[1,2*], Benjamin Sawadogo[1], Kalidou Traoré[3], Urbain Wenmenga[1], Naba Seta[1], Benjamin Allou[2]

[1]Laboratoire Géosciences et Environnement (LaGE), Département des Sciences de la Terre, Université Joseph Ki-Zerbo, Ouagadougou, Burkina Faso
[2]Essakane Sarl, IAMGOLD Corporation, Ouagadougou, Burkina Faso
[3]Laboratoire de Géodynamique et de Cartographie, Université des Sciences, des Techniques et des Technologies de Bamako, Bamako, Mali
Email: *marcvalea@gmail.com

How to cite this paper: Valea, M.D., Sawadogo, B., Traoré, K., Wenmenga, U., Seta, N. and Allou, B. (2024) Structural Pattern Related to Gold Mineralization in the Essakane Area (Northern Burkina Faso, West African Craton). *Open Journal of Geology*, **14**, 855-879.
https://doi.org/10.4236/ojg.2024.149037

Received: July 20, 2024
Accepted: September 17, 2024
Published: September 20, 2024

Abstract

The finite deformation structures recorded in the Essakane area, located in the northeast corner of Burkina Faso, highlight three major compressive deformation phases, successively named D1, D2, and D3. The D1 event phase, trending NE-SW, is characterised by P1 folds and S1 axial plane schistosity. The D2 phase trending NW-SE is characterised by folds P2, schistosity (S2) and shear (C) planes. And the D3 phase trending NNE-SSW to N-S is characterised by P3 folds, crenulation microfolds and S3 spaced schistosity. It has also been noted that gold mineralizations are mainly hosted in quartz, carbonate, pyrite, and arsenopyrite veins. Structural interpretation indicates that these veins are organized into lenticular bodies that were formed during the first two deformation phases (D1 and D2). This suggests a strong structural control typical of orogenic gold concentrations.

Keywords

Burkina Faso, Essakane, Shear Zone, Deformation Phases, Orogenic Gold

1. Introduction

The West African Craton is recognized as one of the world's largest metallogenic provinces, with abundant and various mineral resources [1], making it a major focal point for exploration and mining. Among these various mineral resources, gold has spurred the most intense exploration efforts due to its high value on the

international market over the past decade. With over 1000 tonnes of estimated gold reserves in 2017, West Africa represents the most productive Paleoproterozoic region for gold [2]. Numerous studies on West African gold mineralizations associate them with a Precambrian orogenic episode (orogenic gold), with predominantly structural control [3]-[7]. These mineralizations are primarily found in Paleoproterozoic greenstone belts, with evidence of greenschist and/or amphibolite facies metamorphism [4] [5] [8].

Burkina Faso, located at the heart of the West African Craton, hosts numerous iconic gold mines, such as Essakane, Mana, and Houndé. These gold deposits are located near major regional crustal structures, such as the Ouahigouya and Banfora-Mana shear zones in the west [9] and the Markoye fault in the east. These major crustal openings can extend several tens of kilometers on the surface and reach depths of several hundred meters [10]-[12]. They played a critical role in the formation of major deposits in Burkina Faso and may have served as primary conduits for deep-source hydrothermal fluids. However, despite the influence of regional structures [13], the distribution of gold deposits in the Birimian terrains of West Africa remains quite irregular [14]-[17]. At the deposit scale, other critical metallogenic factors are generally considered, such as lithology, metamorphism, secondary structures (secondary shear zones, folds, tension gashes), and post-mineralization remobilizations.

The Essakane gold mine, located in the northeast of Burkina Faso, at 330 km from Ouagadougou, is the largest gold producer of Burkina Faso, with resources exceeding 6 million ounces and in operation since 2010. This mine and its satellite deposits offer a wealth of information accessible through mining pits and a large amount of exploration drill cores. Thus, the site shows a unique opportunity for detailed structural characterization, allowing the discussion of determining structural factors that control orogenic gold mineralizations in West Africa. This study aims to improve paradigms on the formation mode of orogenic gold deposits and serve as an exploration guide for mining companies.

2. Geological Context of the Study Area

The Essakane gold mine is located in the southern part of the Leo Shield, within the Paleoproterozoic Birimian formations of the Baoulé-Mossi domain (**Figure 1** and **Figure 2**). It is precisely located on a volcano-sedimentary belt known as the Oudalan-Gourouol belt. In terms of lithostratigraphy, it is accepted that at the base of this belt lie early birimian formations, which are unconformably overlain by Birimian Sensu Stricto (S.S.) formations, dated between 2.15 and 1.8 Ga. The early birimian formations are composed of gneisses, migmatites, amphibolites, and leptynites [18]-[21]. The Birimian S.S. formations include a lower series (Lower Birimian), consisting of basalts, gabbros, dolerites, regularly schistose tuffs, and volcanic complexes. Overlying this lower series is an upper series (Upper Birimian) primarily composed of sequences of clastic sediments (polymictic conglomerates, graywackes, siltstones, and argillites) intruded by mafic magmatic

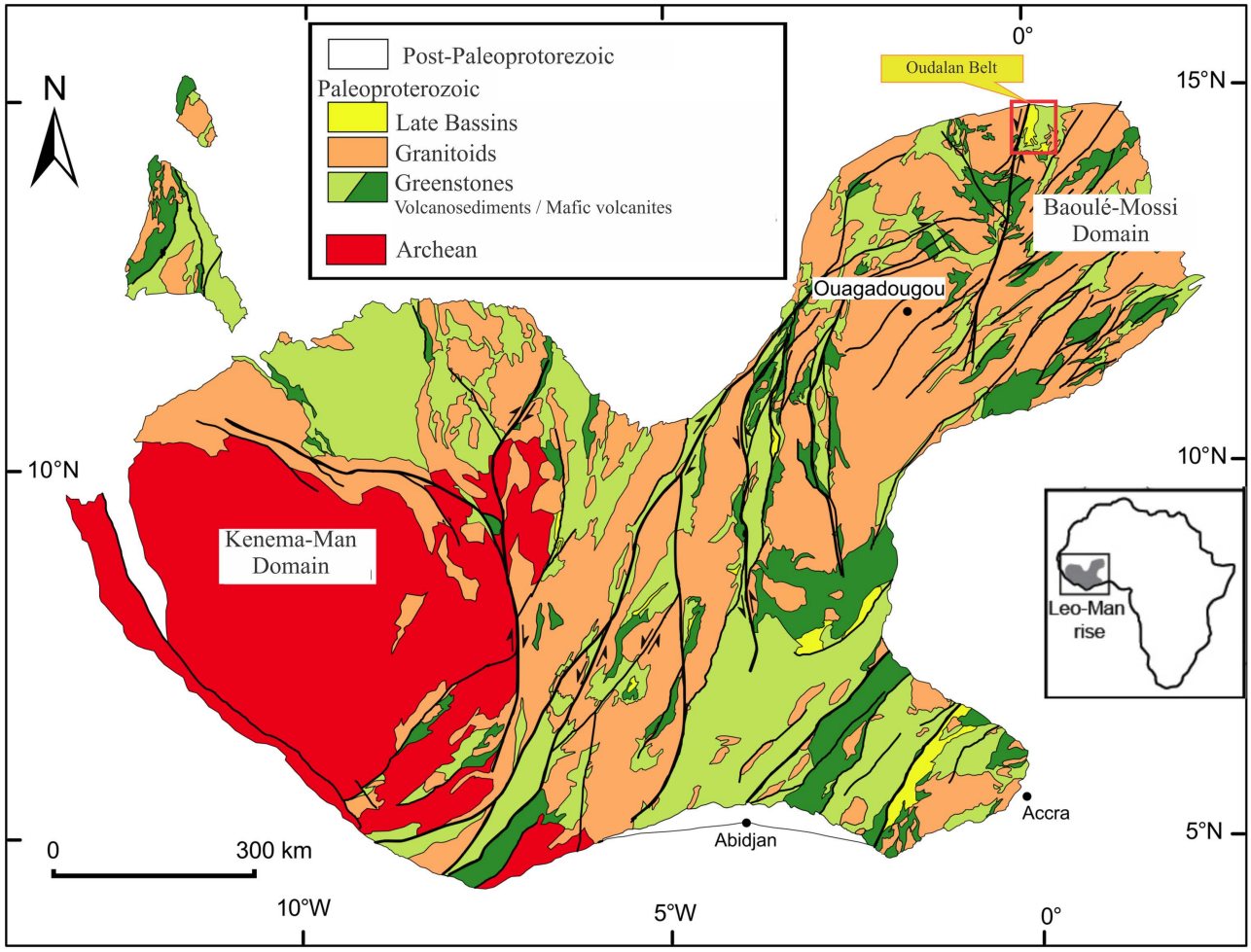

Figure 1. Simplified geological map of the Leo-Man Shield (modified from [15]).

dikes [20]-[23]. Authors such as [3] [4] [8] and [24] have identified Tarkwaian formations within the Oudalan-Gourouol volcano-sedimentary belt, lying unconformably on the birimian formations. These formations are mainly composed of polymictic conglomerates and arkosic quartzites. However, according to the studies of [25] and [23], the sequence defined as Tarkwaian in the Oudalan-Gourouol volcano-sedimentary belt, being lithologically similar to the Upper Birimian, is consequently different from the known and defined Tarkwaian formations in Ghana [3] [4] [26]-[29].

Two phases of deformation were defined by the works of [30] [31] and [23]. The first deformation phase (D1) is characterized by NE-SW-oriented crustal shortening associated with the Tangaean orogeny (2170 to 2130 Ma), while the second phase (D2), also marked by a period of progressive NW-SE-oriented compression, is related to the Eburnean orogeny, which occurred between 2130 and 1980 Ma. The study area is bounded to the west by the Markoye fault (**Figure 2**). This fault has been interpreted in various ways over time in terms of its typology and kinematics. Delfour and Jeambrun [19] attributed it to an east-dipping thrust, while [3] [4] [8], as well as [32], considered it a west-dipping thrust. The

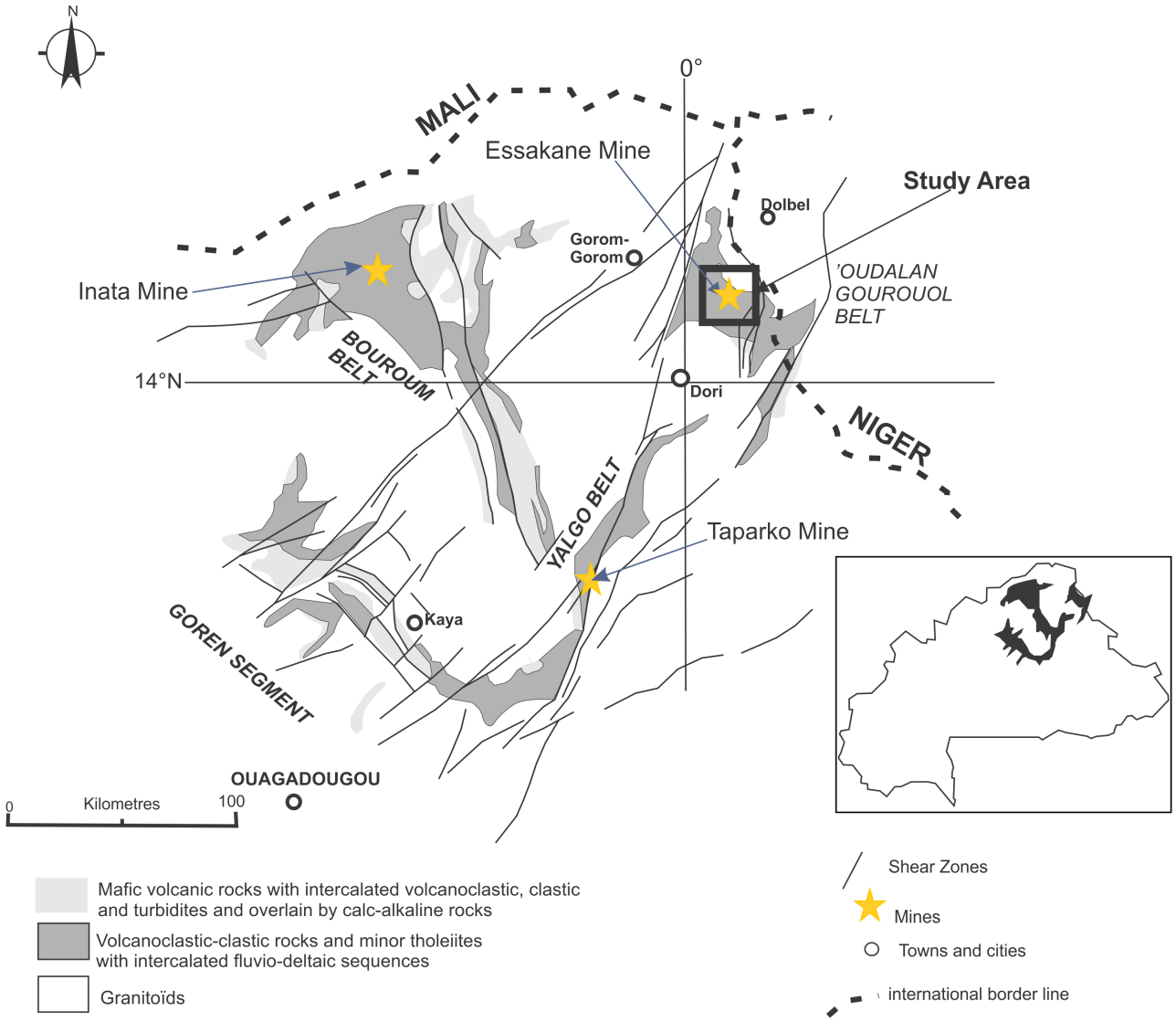

Figure 2. Location of the Oudalan-Gourouol, Bouroum, Yalgo and Goren greenstone belts (modified from [23]).

BHP team, working on the Essakane project in the 1990s [33], characterized it as a regional dextral strike-slip system, while [24] proposed a major sinistral shear zone. These various interpretations deserve a closer examination of the kinematics of the Markoye fault through structures observed in the field.

The volcanosedimentary formations of the Oudalan-Gourouol belt were affected by regional metamorphism, predominantly in the greenschist facies and, more locally, in the amphibolite facies, in relation to the various phases of deformation. The amphibolite facies assemblage is also observed around the granitic intrusions [21] [23] [25].

3. Methodology

3.1. Structural Mapping

Our study began with the analysis of Ikonos panchromatic satellite images (**Figure 3**)

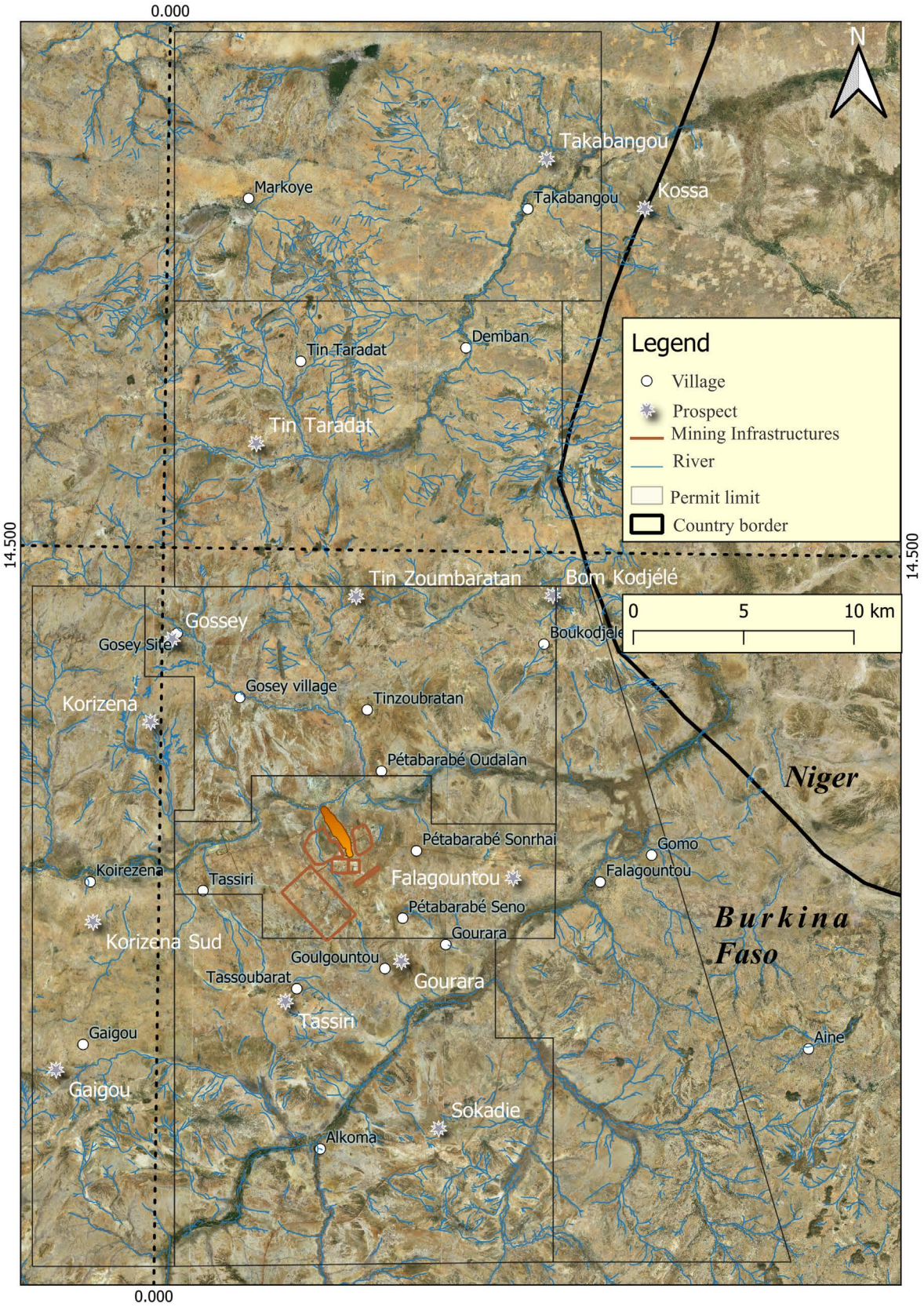

Figure 3. Remote sensing data covering the study area: IKONOS satellite image.

and aeromagnetic maps (analytical signal and first vertical derivative of the total magnetic field reduced to the pole) (**Figure 4**), which provided a synoptic view of several regional structures including mesoscopic folds and kilometer-scale fault deduced by direct tracing of color contrasts. This analysis also guided the field mapping towards potential outcropping areas. During this mapping, geographic positions surveyed by GPS, and all structural measurements were recorded with a Brunton compass using the right-hand rule method. In addition to these field data, structural and lithological informations were measured on drill cores, collected on the project area. The structural data (alpha/beta angles), gathered using goniometer, were then converted into strike and dip using the Target software from Oasis Montaj. Stereographic projections were then created using the Orient software. The type of projection chosen was the lower hemisphere Schmidt projection, and the number of data points was reported using the prefix "N".

3.2. Geochemical Data

The geochemical data used come from several soil geochemistry campaigns conducted by IAMGOLD, following a maximum grid spacing of 400 m × 100 m. The samples were taken from rock using reverse circulation drilling. The gold analyses of the samples were performed at BIGS Burkina laboratory by leaching with atomic absorption spectrometry (AAS) finish. The data processing involved creating contour maps by the minimum curvature method using the Oasis Montaj 8.5 software.

4. Results

4.1. Structural Analysis

Regional folded structures are well highlighted through the interpretation of geophysical data coupled with field observations. These folds, with wavelengths ranging from metric to kilometric scales, are clearly distinguishable between large shear zones that border the east, west, and south of the study area (**Figure 4**). The association of these folds with other identified structures allows them to be distinguished into three main families.

4.1.1. P1 Fold, Axial Plane Cleavage S1, and Thrust Faults F1

The first family of folds (P1) (**Figure 5** and **Figure 6**) is characterized by subvertical axial planes striking NW-SE to NNW-SSE with subhorizontal fold axis. Along these axial planes, a very discrete axial plane cleavage S1 develops locally, observed mainly in the mining pit and trenches over the Essakane deposit. This family of folds, with wavelengths ranging from hectometric to kilometric scales, is easily observable in several locations: 1) in the Essakane pit (**Figure 6(A)** and **Figure 6(B)**); 2) 10 km north of the Essakane deposit near the village of Tin Zoumbaratan, where it is marked by a syncline-anticline succession with kilometric-scale wavelengths (**Figure 4**); 3) 5 km southwest of Essakane near Tassiri, where it is difficult to observe due to alluvial cover but can be easily interpreted from core

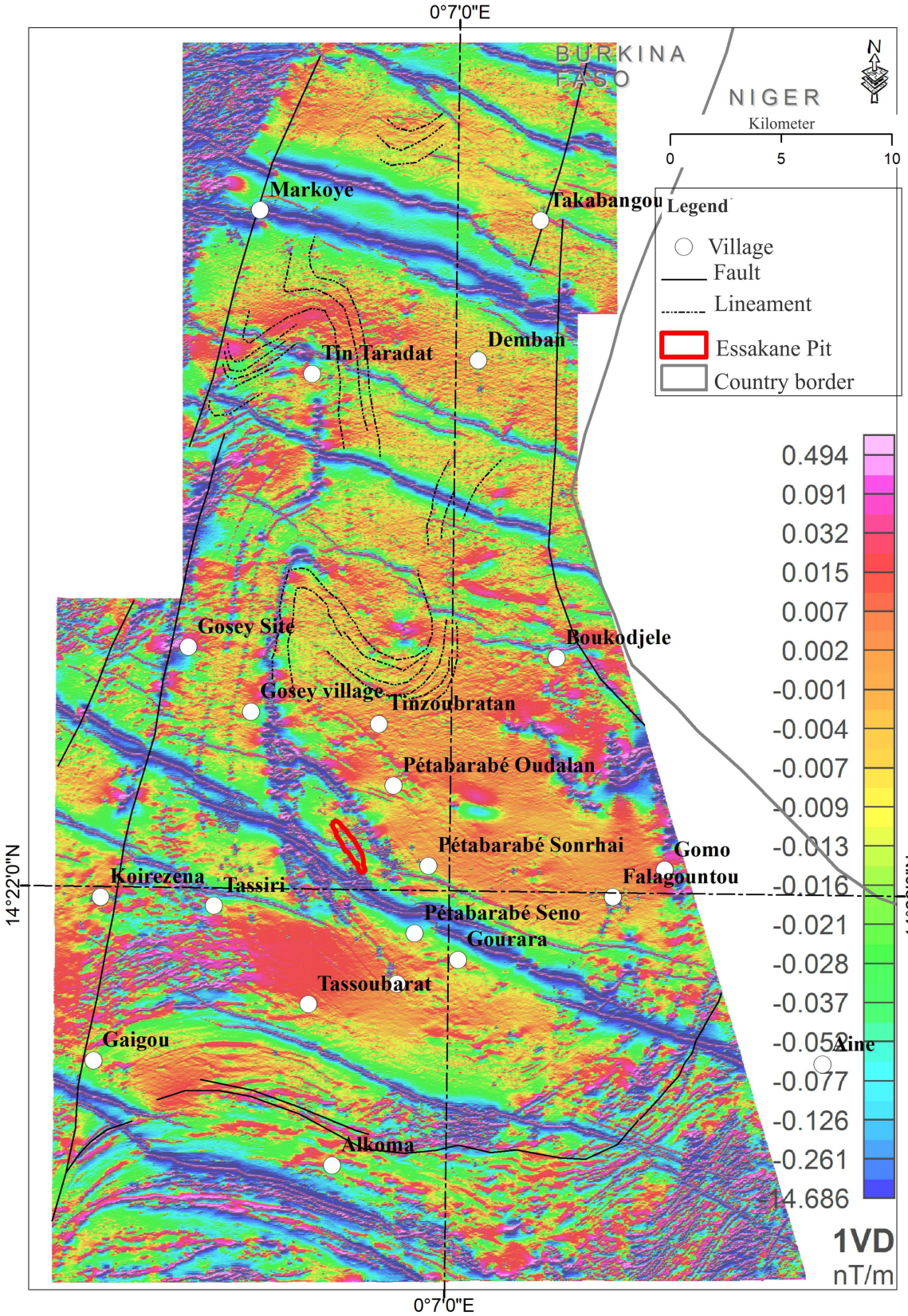

Figure 4. Remote sensing data covering the study area: first vertical derivative of the total magnetic field reduced to the pole, in color and shaded relief.

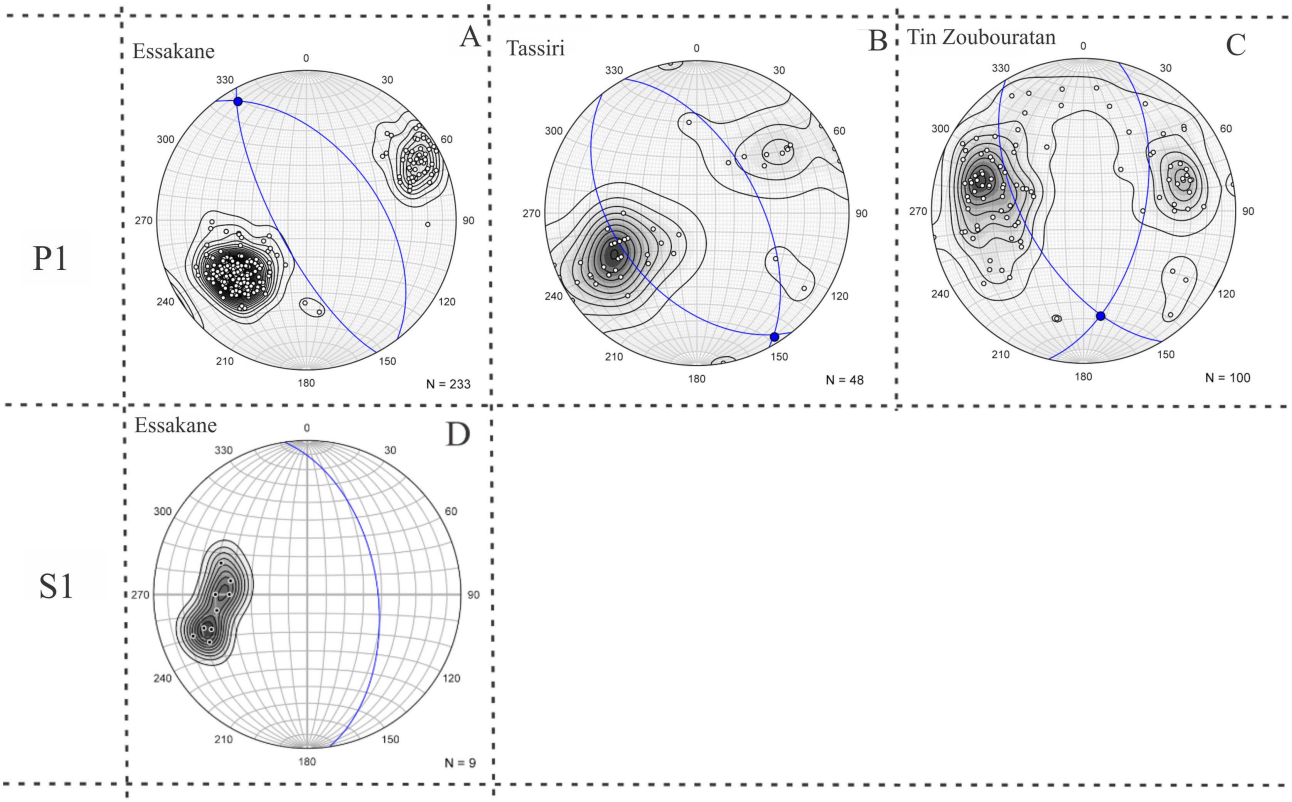

Figure 5. Schmidt orientation diagram (lower hemisphere) of the main D1 structures: (A) Bedding planes (S0) at the Essakane anticline: mean fold axis: N329˚/10˚; (B) Bedding planes (S0) at the Tassiri anticline: mean fold axis: N147˚/06˚; (C) Bedding planes (S0) at the folded structure of Tin Zoumbaratan: mean fold axis: N171˚/31˚; (D) Axial plane schistosity (S1) of the Essakane fold: mean plane N352˚/52˚E.

drillings conducted in the area; 4) 14 km northeast near Bom Kodjélé, where it is characterized by an asymmetric fold verging southwest, intersected by a thrust fault dipping slightly eastward (**Figure 4**).

The geometry of the Essakane deposit, exposed in the pit, allowed for a more detailed study of the tectonic structures associated with the P1 fold family. Thus, this geometry corresponds to an asymmetric anticline verging westward, affected by a system of thrust faults dipping eastward (**Figure 6(A)** and **Figure 6(B)**). Analysis of the orientation diagram of bedding planes measured at the Essakane pit allows for the interpretation of an overturned fold with an average opening angle of 56˚ (close fold according to [34]) and a plunging axis of 10˚ towards N329˚ (**Figure 5**(A)).

The average attitude of the limbs is N321˚/51˚E for the eastern limb and N153˚/73˚E for the western limb, and the axial plane is inclined 80˚ to the east. Thus, all the geometric characteristics of this fold (P1) allow for the determination of an average direction of maximum stress $\sigma 1$ at N059˚-N239˚ (NE-SW).

The thrust faults (**Figure 6(A)** and **Figure 6(B)**) have an average orientation of NW-SE (N322˚, 48˚E), very close to that of the stratigraphic layers on the eastern limb. In the mining pit, these faults generally follow interbedded planes in the sedimentary sequences or intersect them at a low angle with either the dip

or the strike. The displacements observed on these faults appear to be minor, on the order of a few meters at most. Two sets of NE-SW striking faults (perpendicular to the main fold axis) with opposite dips are observed on the western wall of the Essakane pit (Figure 5(C) and Figure 5(D)). These faults exhibit apparent displacement characterized by reverse movements on subvertical tension veins cogenetic with the Essakane fold. These faults would then fit perfectly into a second phase of compression parallel to the axis of the Essakane fold (NW-SE) and generating the P2 folds.

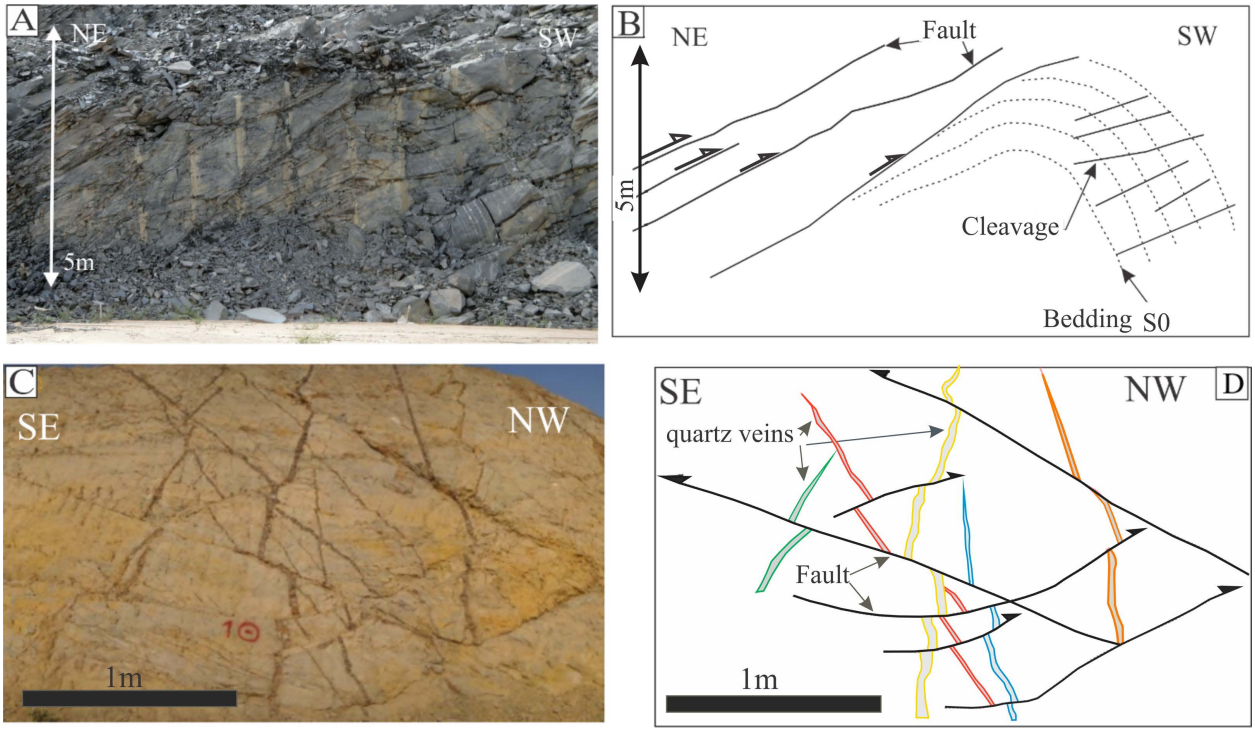

Figure 6. Deformation markers on the Essakane deposit: (A) Southeast view of the fold hinge (P1); (B) Interpretation of photo (A); (C) West wall of the Essakane pit (view towards the southwest), with apparent displacement on the veins due to the action of conjugate reverse faults; (D) Interpretation of photo (C).

4.1.2. P2 Fold, Cleavage S2, S2-C, and Shear Zone

- **P2 Fold**

The second family of folds (P2; Figure 7), highlighted in the field by the variation in dip directions, is characterized by axial planes striking NE-SW to NNE-SSW. These planes host gently plunging fold axis towards the NE. These folded structures, at kilometric-scale, are also clearly observed from aeromagnetic images, notably in Tin Taradat, and Gossey, towards the village of Markoye, and west of Bom Kodjélé (Figure 4). Large deformation corridors extending over several kilometers are associated with these P2 folds.

- **Gossey-Korezina Shear Zone**

The Gossey-Korezina deformation corridor, located to the west of the study area, exhibits a main NNE-SSW direction. This corridor is marked by structural discontinuities such as WNW-ESE striking faults generally filled by dolerite

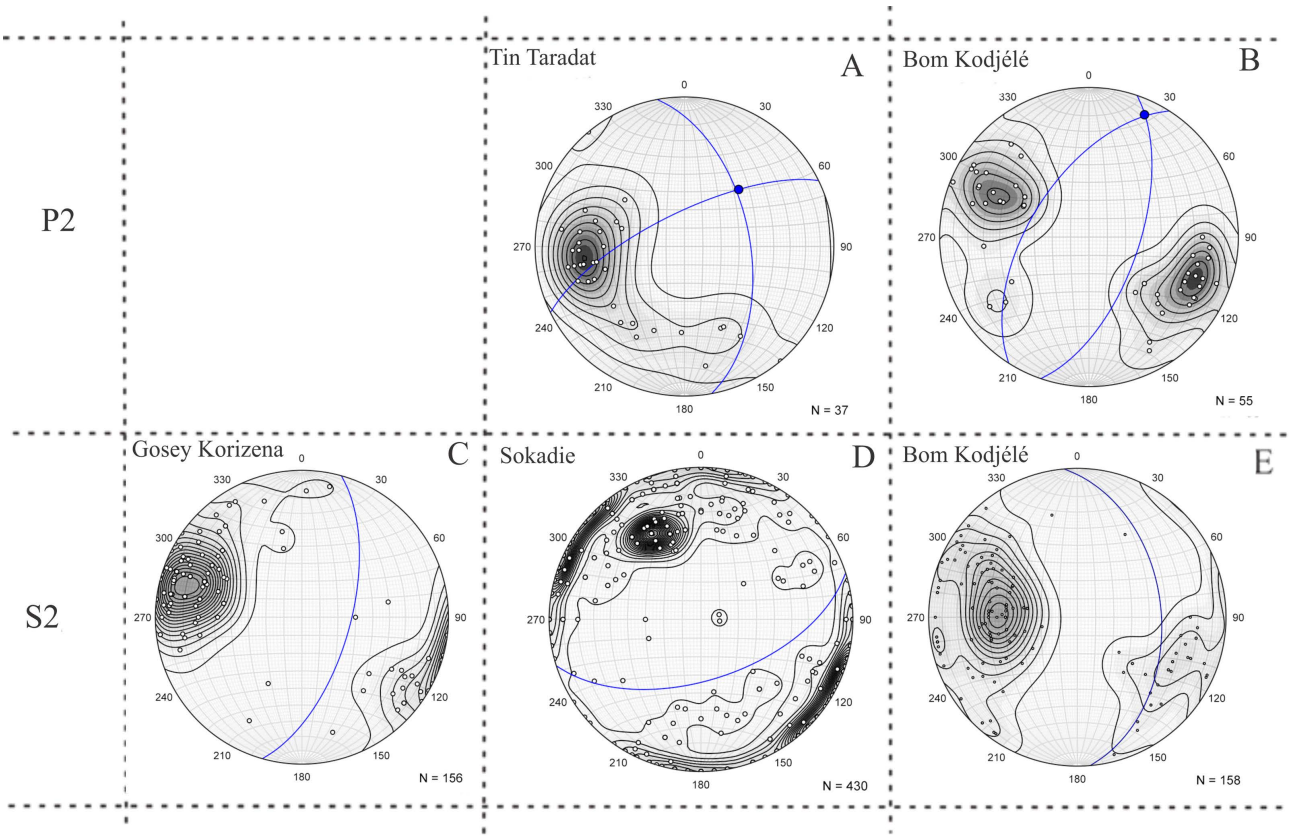

Figure 7. Schmidt orientation diagram (lower hemisphere) of bedding planes (S0) for: (A) Folded structure of Tin Taradat; calculated fold axis: N043˚/47˚; (B) Folded structure west of Bom Kodjélé; calculated fold axis: N024˚/10˚; ((C)~(E)) S2-C planes measured on the shear zone of Gossey-Korezina, Sokadie, and Bom Kodjélé, respectively.

dykes. It is also intersected by quartz veins with decametric thicknesses (**Figure 8(A)**) and directions ranging from N10˚ to N40˚. These veins, which are sometimes parallel to the shear corridor, exhibit a brecciated structure characterized by crushed quartz within a siliceous cement. This could be evidence of the early nature of these veins. The main deformation fabrics observed in this corridor are cleavage (S2) and shear (C) planes, often merged (**Figure 8(B)**) and parallel to the bedding (S0). Stereographic analysis of cleavage measurements, conducted both in the field (**Figure 7(C)**) and more locally on oriented drill cores, yields an average orientation of N19˚/72˚E and N15˚/65˚E, respectively. The regolith cover makes bedding measurements in the field very difficult, so that only the measurements collected on oriented drill cores were considered. Their analysis gives an average orientation of N14˚/66˚E.

A more detailed zonal analysis of these planes (S0, S2-C) reveals a progressive flexure in orientations, ranging from NNE-SSW with a mean dip of 60˚E in the north of the corridor, to NE-SW with sub-vertical dips towards the south.

In addition to this cleavage, other deformation structures can also be observed in places, such as asymmetric boudinaged quartz veins, en echelon tension veins (**Figure 8(C)**), sigmoidal clasts (**Figure 8(D)**), and metric wavelength isoclinal folds with vertical axis and axial planes parallel to the deformation corridor. The

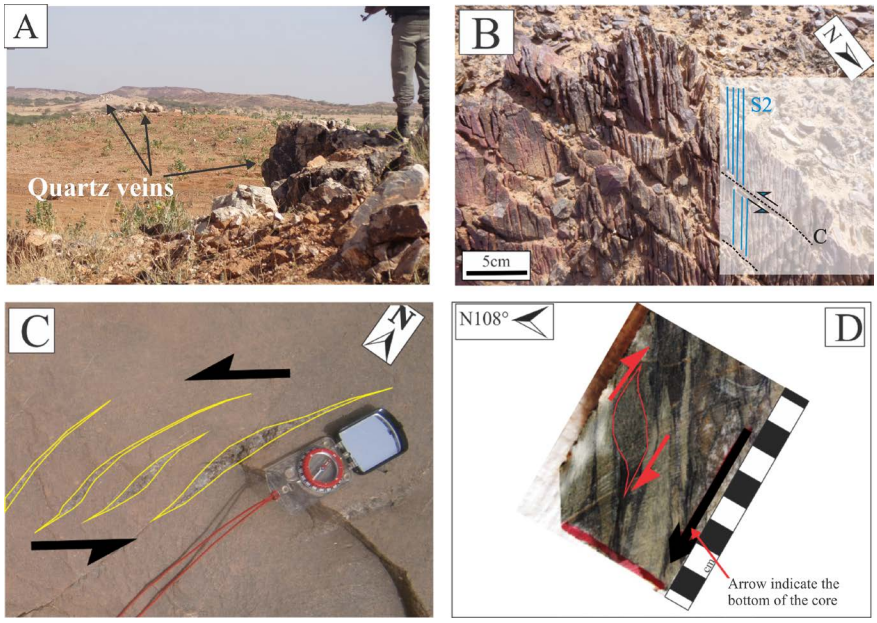

Figure 8. Deformation markers in the Gossey-Korizena shear zone: (A) Quartz veins oriented N20˚E, observed within the shear zone; (B) Subvertical cleavage with a direction of N34˚E, observed in detrital metasediments within the deformation corridor; (C) Tension veins with an average direction of N20˚, arranged en echelon in lithic sandstone indicating sinistral strike-slip shearing; (D) Sigmoidal clast within detrital metasediments (microconglomerate) indicating reverse movement inclined eastward, on an oriented drill core (Hole n˚: KDD0036 drilled at N108˚/60˚).

geometric characteristics of these structures suggest non-coaxial deformation characterized by an NNE-SSW to NE-SW shear with a dominant reverse-sinistral component and an eastward dip.

- **Sokadie Shear Zone**

The Sokadie shear zone, located south of the Essakane mine, borders the northern contact of the Dori granite. This structure has an overall E-W direction, which tends to curve southwards at its western end and northwards at its eastern end (**Figure 4**). It is intersected by brecciated quartz veins characterized by crushed quartz within a siliceous cement, identical to those observed along the Gossey-Korezina shear zone. These veins are subvertical, with orientations ranging from N80˚ to N110˚.

The main deformation structures observed in this corridor are represented by S2-C planes, which are very often merged (**Figure 9(A)**). These planes (S2 and C), dipping slightly to the south, and are parallel to the bedding. Statistical analysis of the schistosity planes, based on orientation diagrams, shows an average orientation of N72˚/57˚S for measurements collected at outcrops (**Figure 7(D)**) and N81˚/52˚S for measurements collected from oriented drill core. The bedding measurements collected from oriented drill cores give an average orientation of N88˚/55˚S. The relationship between the cleavage and shear planes (**Figure 9(C)** and **Figure 9(D)**), the asymmetrical appearance of microfolds observed on the oriented drill cores, and the asymmetric pressure shadows around certain minerals (**Figure 9(B)**)

define a shear zone characterized by a dextral-normal movement in an E-W direction.

A plan view observation of the NNE-SSW (Gossey-Korezina) and E-W (Sokadie) striking shear corridors, which are respectively sinistral and dextral, suggests contemporaneity in their formation. These two corridors thus form a conjugate structure resulting from the same compression.

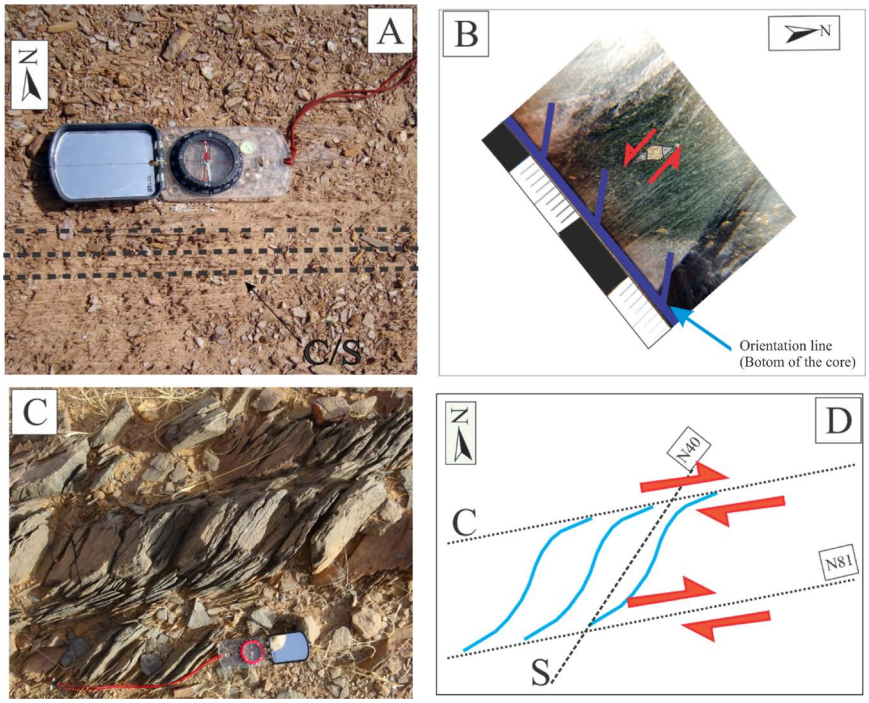

Figure 9. Deformation markers in the Sokadie shear corridor: (A) C planes parallel to S planes with an E-W orientation within mica schist; (B) Asymmetric pressure shadow around pyrite within diorite, indicating normal movement on an oriented drill core (Hole n˚: SDD0032 drilled at N360˚/60˚); (C) C/S planes observed within detrital sedimentary formation indicating dextral strike-slip shearing in an E-W direction; (D) Interpretation of photo (C).

- **Bom Kodjélé and Takabangou Shear Zones**

The deformation corridor to the east of the study area is marked by a local offset of dolerite dykes (**Figure 4**). The northern part (Takabangou structure) of this corridor appears to shift westward with a rotation of approximately 30˚. The southern part (Bom Kodjélé structure) is mainly oriented NNW-SSE to N-S, while the Takabangou portion (northern part) has an NNE-SSW direction. On the Bom Kodjélé structure, the lithological formations observed are affected by penetrative cleavage (S2-C) (**Figure 10(A)**). This cleavage is characterized by shear planes appearing occasionally subparallel to the rarely preserved bedding (S0) (**Figure 10(B)**). The average orientation of the cleavage is N354˚/41˚E (**Figure 7(E)**). A more detailed analysis indicates a change in the appearance of these structures on either side of the fault. They transition from a strongly eastward-inclined N-S direction to a more upright NNE-SSW direction, respectively to the east and west of the fault.

The observation of boudinaged veins, slip striations (Figure 10(C) and Figure 10(D)), and the asymmetrical appearance of some microfolds indicate that the Bom Kodjélé deformation corridor is an oblique N-S shear zone dipping eastward, characterized by predominantly sinistral reverse movements.

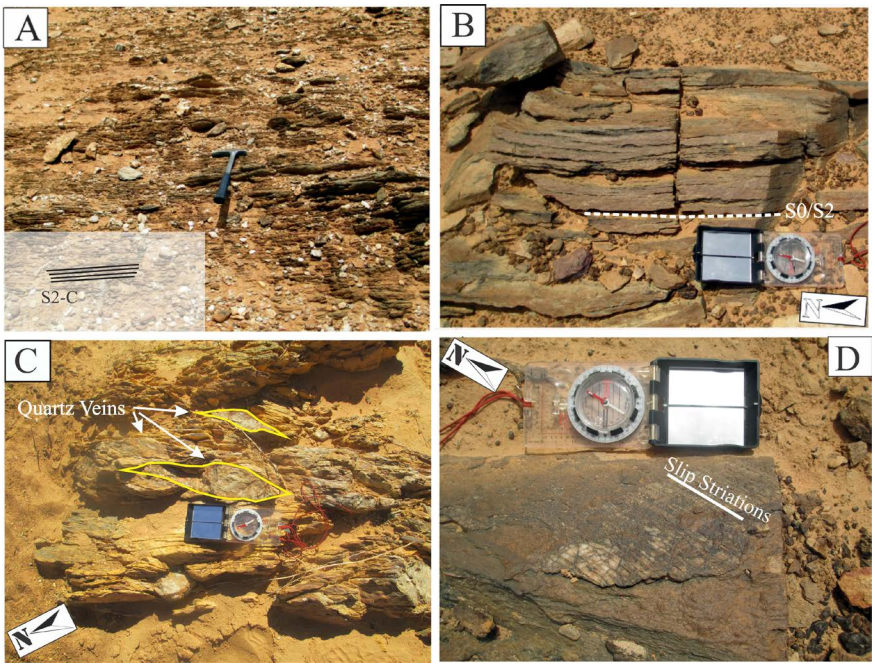

Figure 10. Deformation markers in the Bom Kodjélé shear zone: (A) C plane parallel to S plane (S2-C) with an N-S orientation within micaschist observed on the Bom Kodjélé shear corridor; (B) S2 slaty cleavage transposed onto the bedding (S0) within detrital sedimentary rocks south of Bom Kodjélé; (C) Boudinaged quartz veins, oriented NE-SW; (D) Slip striations observed on the Bom Kodjélé deformation corridor.

4.1.3. P3 Fold and Spaced Cleavage S3

A third family of folds (P3), more discreet, is very difficult to observe from airborne magnetic images. However, field observations define folds characterized by axial planes, oriented E-W carrying subvertical fold axis. They have a metric-scale wavelength (Figure 11(A) and Figure 11(B)) and are associated with spaced cleavage (S3) oriented N70˚ to N90˚, characterized by crenulations and fractures with sinistral micro-displacements (Figure 11(C) and Figure 11(D)). These folds are observed very locally at the extreme east and west of the study area within volcanosedimentary formations.

4.2. Gold Mineralization

Most of the gold occurrences in the study area were already known and exploited by artisanal miners. Analysis of soil geochemistry data has highlighted several gold anomalies, most of which are in line with the deformation structures of various orders defined in the study area and include artisanal mining sites (Figure 12). These sectors with geochemical anomalies consistent with structural directions actually organize around the main deformation corridors described earlier,

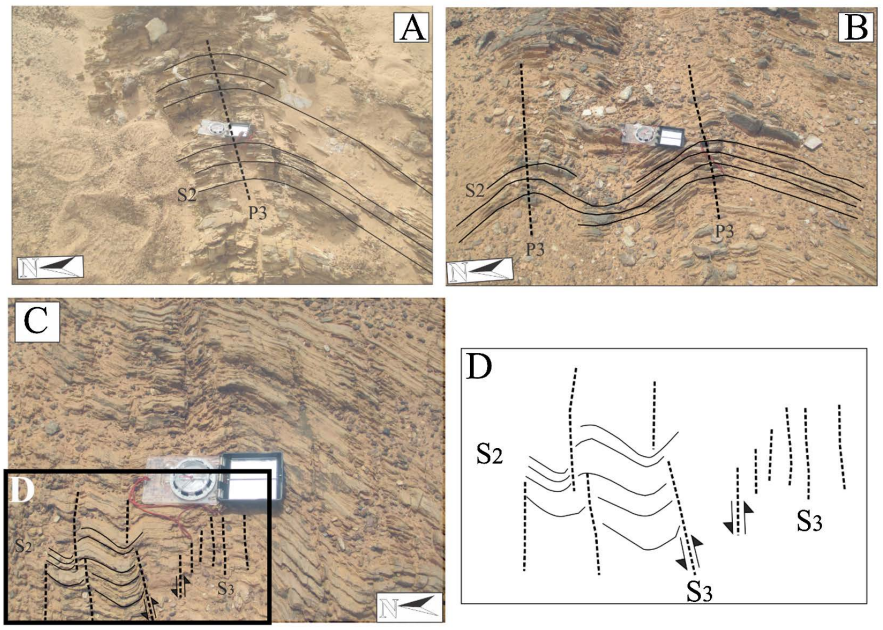

Figure 11. Late deformation markers (D3): ((A) (B)) Metric-scale fold (P3) with E-W oriented axial planes and subvertical fold axis; (C) Bom Kodjélé deformation corridor-oriented N-S (S2) affected by crenulation cleavage (S3) oriented E-W with sinistral micro-displacements; (D) Interpretation of a portion of photo (C).

in addition to the Falagountou deposit and those associated with folded structures.

4.2.1. Gold Mineralization Associated with the Gossey-Korezina Shear Zone

The geochemical anomaly pattern perfectly circumscribes the Gossey-Korezina shear corridor and appears to follow the limb of a more northern anticline at the Tin Taradat prospect (**Figure 12**). The anomaly is more dispersed south of Korezina and seems to follow the virgation induced by mafic intrusions. This shear zone hosts the gold occurrences of Gossey-Korezina to the north and Gaigou to the south. The Gossey-Korezina occurrence, as its name suggests, connects the prospects of Gossey and Korezina and is located approximately 10 km northwest of the Essakane mine. It is characterized by gold mineralization hosted by subvertical linear and lenticular bodies, formed by stockworks of veins (millimetric to centimetric) filled with quartz accompanied by varying amounts of carbonates, sericite, chlorite, pyrite, and arsenopyrite. The mineralization follows a main direction of N10˚, with a secondary direction of N35˚. It is hosted within a polygenic microconglomeratic sandy sedimentary formation in contact with mafic to intermediate intrusive rocks.

4.2.2. Gold Mineralization Associated with the Sokadie Shear Zone

The Sokadie occurrence is located approximately 13 km south of the Essakane deposit and follows the E-W Sokadie shear zone (**Figure 12**). The gold mineralized zone is characterized by cataclastic veins and hydrothermal breccias composed of quartz accompanied by varying amounts of carbonate, pyrite, chlorite,

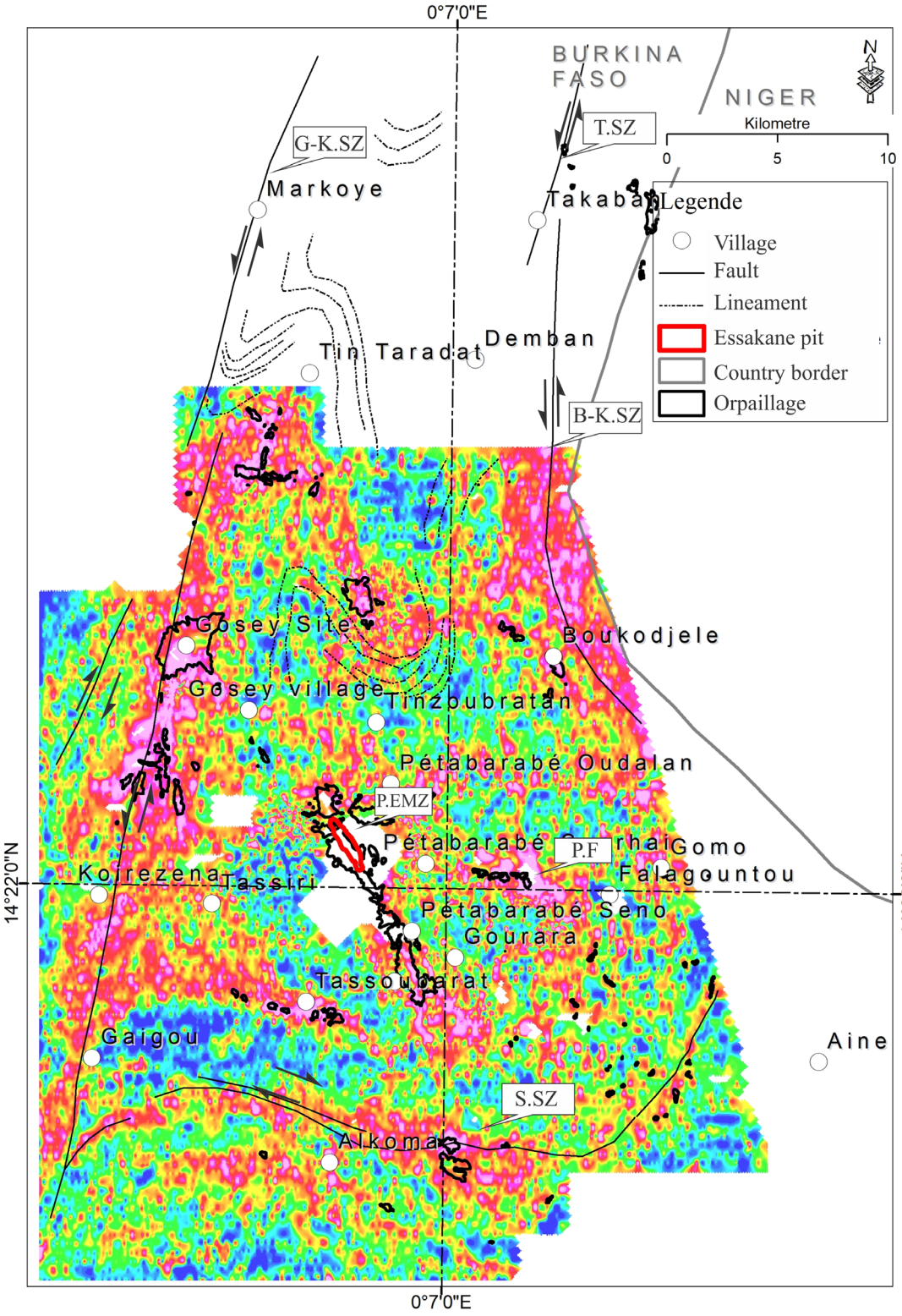

Figure 12. Distribution of geochemical anomalies for gold based on the results of soil geochemistry sample analyses (interpolation method: minimum curvature) on the Essakane SARL permits: P.EMZ: Main pit of Essakane, P.F: Satellite pit of Falagountou, S.SZ: Sokadie Shear Zone, B-K.SZ: Bom Kodjélé Shear Zone, G-K.SZ: Gossey Korizena Shear Zone, T.SZ: Takabangou Shear Zone. The map uses color coding where pink indicates the highest concentrations and blue indicates the lowest concentrations of gold.

tourmaline, sericite, and magnetite. These centimeter-thick veins are organized into stockwork lenses ranging from decametric to hectometric size, hosted within a highly deformed dioritic intrusive rock. These lenses have a main direction of N80˚ and a secondary direction of N110˚, with a steep southward dip.

4.2.3. Gold Mineralization Associated with the Bom Kodjélé Shear Zone

The Bom Kodjélé gold occurrence is located 14 km northeast of the Essakane deposit at the extreme eastern part of the study area. It is hosted by the NNW-SSE to N-S Bom Kodjélé shear zone and is perfectly highlighted by a geochemical anomaly (**Figure 12**). The mineralization is found within highly deformed volcanosedimentary rocks in contact with mafic to intermediate intrusive rocks. It is hosted by quartz and quartz carbonates veins (centimetric to decimetric) of, which are brecciated, ribboned, sheared, and sometimes boudinaged, with gold associated with pyrite, arsenopyrite, and occasionally chlorite. These hydrothermal veins and breccias have an average orientation of NNE-SSW (N30˚) and are arranged en echelon along the NNW-SSE reverse fault.

4.2.4. Falagountou Deposit

The Falagountou deposit, located 7 km east of the Essakane mine, is covered by a thick layer of aeolian sand (approximately 15 m), which would have reduced its surface geochemical signature if the soil geochemistry survey had not been conducted with varying depths according to the thickness of the regolith (**Figure 12**). The mineralization is primarily characterized by quartz veins accompanied by carbonates, chlorite, arsenopyrite, pyrite, and chalcopyrite, organized into stockworks and located at the contact of mafic intrusions with equigranular to porphyritic textures, with feldspar phenocrysts (porphyritic gabbro), and turbiditic sediments (alternating sandstone, siltstone, and mudstone). Disseminated mineralization is also observed in both the intrusion and the sediments crossed. The general orientation of the mineralization is NNW-SSE (approximately N160˚), with a slight dip towards the east.

4.2.5. Essakane Deposit

The Essakane deposit is characterized by a stockwork of quartz and quartz-carbonate veins accompanied by varying amounts of arsenopyrite, pyrite, pyrrhotite, and chlorite. These veins are hosted within a folded and faulted turbiditic sequence (faulted fold), showing an alternation of arenites and argillites. Gold is observed in free form within the veins or associated with arsenopyrite at the vein margins. Disseminated gold is also present in the host rock but at very low grades. The competence contrast between fine-grained argillites and more brittle arenites controls the orientation and continuity of the vein networks hosting the gold mineralization. The most mineralized zones are primarily located where east dipping thrust faults cross the fold hinge, as well as on the eastern limb of the fold. The Essakane deposit's stockwork comprises several vein families (**Figure 13**), with the main types being: 1) Laminated (sheared) veins and 2) tension veins

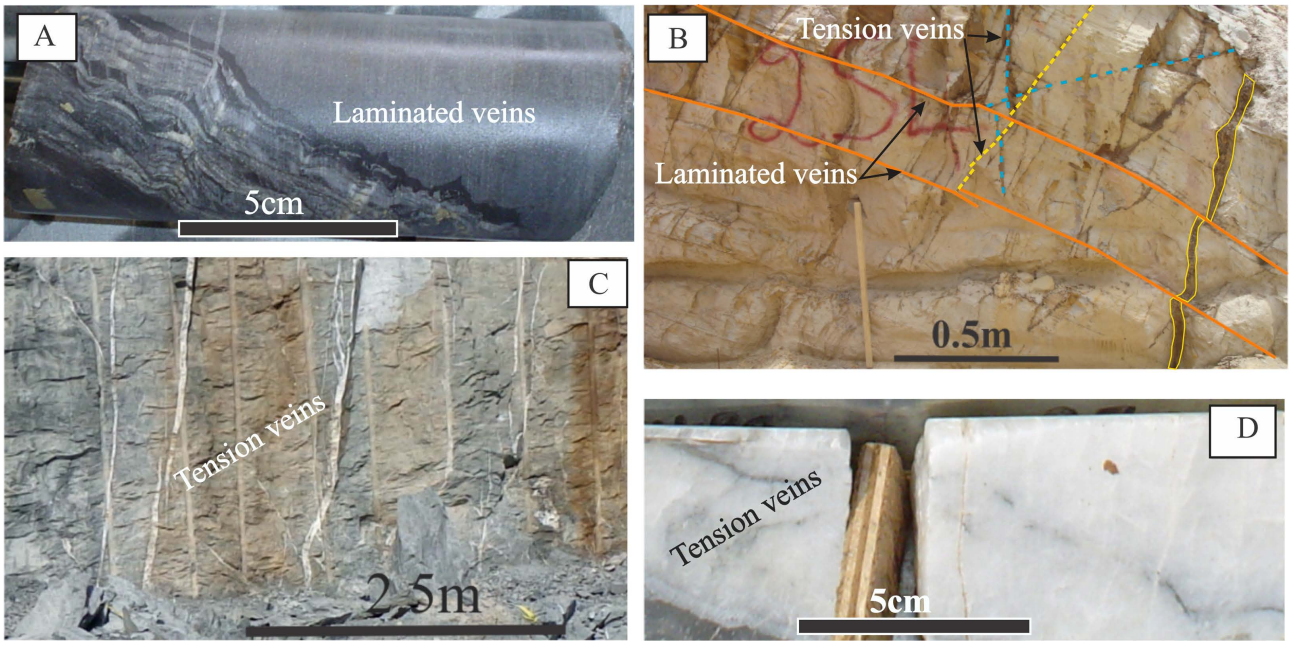

Figure 13. Quartz veins observed in the Essakane Anticline: (A) Laminated vein (core photo); (B) View looking northwest of a trench with bedding-parallel veins intersecting subvertical veins parallel and oblique to the main Essakane fold axis; (C) View looking east of a wall in the Essakane pit with subvertical tension veins perpendicular to the fold axis; (D) Tension veins with massive texture (core photo).

(axial, oblique, and transverse).

- **Laminated Veins**

Laminated veins parallel to the stratification are most commonly observed at the boundary between two sedimentary units and within silt-clay units. These veins consist in layers of quartz ± carbonate ± arsenopyrite veinlets alternating with sheared host rocks (**Figure 13(A)**). They occur at all levels of the Essakane fold (limbs and hinge) and can be observed either displacing or being displaced by steeply dipping veins parallel to the fold axis (**Figure 13(B)**). The quartz in these veins is distinctive due to its gray color. Gold grades in these veins are generally low (<5 g/t).

- **Tension Veins**

Axial tension veins are parallel to the fold axis and arranged in a symmetrical fan across the fold hinge, while transverse veins are subvertical and oriented perpendicular to the fold axis. These veins are well developed in the less ductile arenitic units. Both families of veins (axial and transverse) have been extensively mined by artisanal miners due to the thickness of their walls and their persistent direction. They appear white (**Figure 13(C)** and **Figure 13(D)**), in contrast to the gray color of the laminated veins, and generally have the highest gold grades, reaching up to 100 g/t. Shear joint systems (conjugate structures formed from oblique fractures) consistently develop along the fold limbs. These structures are less developed and therefore less likely to be conduits for hydrothermal fluids.

5. Discussion

5.1. Different Phases of Deformation

The structural synthesis of the tectonic fabrics observed in the study area indicates that it has undergone multiple compressive tectonic events (Table 1), with the first two being perpendicular to each other.

Table 1. Structural scheme of the study area. TF: Thrust Fault; TAS: Tassiri; ESK: Essakane; BK: Bom Kodjélé.

Deformations	Structures
D3, N-S shortening Metric scale fold (P3), Axial planes E-W with subvertical fold axis, S3 subvertical in an E-W direction, Minor sinistral displacement	
D2, NW-SE shortening Kilometric scale fold (P2), Axial planes NNE-SSW and NE-SW with subhorizontal fold axis, Reverse-sinistral shear NNE-SSW and N-S, Normal-dextral shear E-W, S2-C planes steeply dipping towards ESE, E, and S	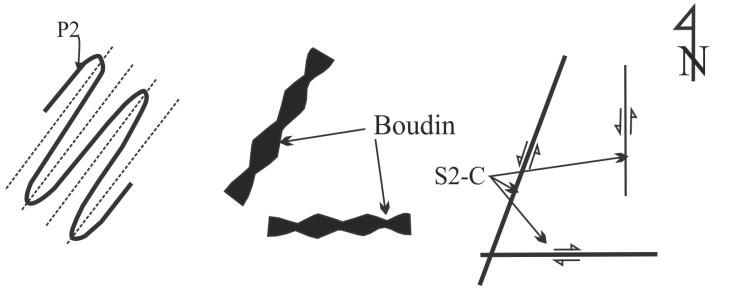
D1, NE-SW shortening Hectometric to kilometric scale fold (P1), Axial planes NW-SE and NNW-SSE with subhorizontal fold axis, S1, subvertical, very discrete, Thrust fault NW-SE and NNW-SSE, Tension veins NNE-SSW to NE-SW	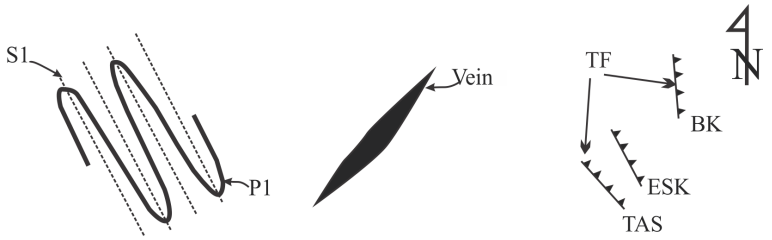

The first phase of deformation (D1), characterized by a ductile-brittle nature, is marked by quartz veins and veinlets representing tension gashes-oriented NNE-SSW to NE-SW. And asymmetric folds (P1), often faulted, with generally subvertical axial planes bearing subhorizontal fold axis-oriented NW-SE to NNW-SSE (Tassiri, Essakane, Tin Zoumbaratan) are observed. The axial planar cleavage (S1) is very discrete and observed locally. The geometric and kinematic interpretation of these structures defines a D1 deformation phase characterized by a major principal stress ($\sigma 1$) oriented NE-SW.

This deformation could be associated with a pre-Eburnean event known as the Tangaean in Burkina Faso, dated to approximately 2170 - 2130 Ma, [31] and Eoeburnean in northern Ghana [35]. The western branch of the Markoye shear zone with a dextral-reverse displacement would correspond to a regional marker of this tectonic event [23].

The second phase of deformation (D2) lead to the refolding of pre-existing P1 folds and the formation of a second family of folds (P2) with axis, oriented NNE-SSW. An example of this is the anticlinal-synclinal sequence that contains the gold indicator at Tin Taradat. The shearing nature of this deformation is easily observable in the field. It is expressed by the relationship between cleavage (S2) and shear (C) planes, by the shape of sigmoidal structures, and pre- to syn-D2 asymmetric boudinaged veins observed within the various deformation corridors of the area. The set of markers, indicate a sinistral reverse movement along the Korezina-Gossey deformation corridors (eastern branch of the Markoye fault), Bom Kodjélé, and a normal dextral movement along the Sokadie deformation corridor. These movements fit perfectly into a conjugate fault system resulting from NW-SE transpression. While horizontal movements are easily observable in the field, vertical movements, on the other hand, had to be revealed from oriented core drilling. This second phase of deformation (D2), characterized by a major principal stress (σ1) oriented NW-SE, is associated with the Eburnean orogeny, dated approximately 2130 - 1980 Ma [23] [30] [31].

The third phase of deformation (D3) is less marked in the field than the first two. It is characterized by its ductile-brittle nature and by a generally N-S to NNE-SSE compression resulting in the formation of a spaced cleavage (S3) of crenulation and fractures accompanied by sinistral micro-displacement oriented N70˚ to N90˚ (WNW-ESE to E-W). These microfolds and fracture cleavage refold and/or cut across the previous S2 cleavages. Metric-scale folds with axial planes parallel to S3 and subvertical axis are also observed. A deformation phase with a similar orientation but rather brittle in nature had previously been identified in northern Burkina Faso in the Goren belt by [31] and [36] and to the northeast in the granitic terrains of Gorom-Gorom (western part of the Markoye fault) by [37].

5.2. Control of Mineralization

At the scale of the study area, gold mineralization is hosted in a variety of lithologies including turbiditic sediments, sandstones, polygenic microconglomeratic sandstones, and intrusions of intermediate to mafic composition. It occurs along structures (folds and faults) oriented NNW-SSE (Essakane, Tassiri), N-S (Falagountou), NNE-SSW (Korizena, Gossey), and E-W (Sokadie). This situation corresponds to epithermal to mesothermal gold deposits, which often exhibit control by faults and are hosted by igneous rocks, as well as sedimentary rocks [38]. Furthermore, as observed in the study area, these types of deposits consist of stockworks or hydrothermal breccias in mineralized host rocks. These breccias and stockworks are emplaced due to significant stress as well as the rheological contrast at lithological contact zones.

At the scale of the Essakane deposit, it appears that regardless of the present lithologies, the highest concentrations of gold are associated with stockwork zones primarily located on the eastern limb, which is more inclined (~60˚E) than the western limb, and at points where the hinge is intersected by reverse faults also inclined

towards the east.

5.3. Timing of Gold Mineralization

In the shear zones of Gossey-Korezina and Sokadie, the mineralized veins observed are brecciated or boudinaged, with principal directions parallel to these zones (N10˚E to N35˚E and N80˚E). This suggests early to syn-tectonic mineralization during the D2 deformation phase (pre- to syn-D2). At the Bom Kodjélé prospect area, the mineralization appears to be earlier, as it is hosted by veins with brecciated or boudinaged structures too, oriented N20˚E to N40˚E, which cut across the deformation zone-oriented NNW-SSE. The emplacement of these veins would then be D1, implying possible mineralization synchronous with D1 (syn-D1).

At the scale of the Essakane deposit (P1 fold), a vein network has been identified that can be described as an "organized" stockwork consisting of several directional families. The two main types of veins observed are laminated (sheared) veins and tension veins.

There is controversy regarding the origin of veins parallel to stratification, despite the subject being addressed by numerous authors such as [39]-[45]. Some authors, such as [39], suggest that veins parallel to stratification can form in an extensional context early in the formation of a basin (post-lithification, during burial) or by late hydrothermal fluid circulation (post-folding hydrothermalism) [40]. However, most studies systematically associate them with a compressive tectonic context. Among these, some suggest that these veins can form early in a fold's history (pre-folding) by developing overpressure zones in impermeable beds during bedding-parallel shortening [41]-[43] [46] or during sliding parallel to bedding during bedding-parallel shortening [47]. Others, such as [48]-[50] and [44], place them in a syn-folding period characterized by fluid circulation along weakness planes developed during folding by sliding and flexing. Finally, [51] considers them as extensions in fold limbs of reverse faults cutting through fold hinges (late- to post-folding). In the Essakane context, the presence of these laminated or sheared texture veins suggests syn- to late- or post-deformation (D1) mineralization.

The extension structures have been studied by several authors, such as [48] [52]-[56]. According to these authors, they result from hinge deformation, expressed by extension compression respectively at the extrados-intrados during a folding phase. These veins can be parallel or perpendicular to the fold axis. According to [48] and [56], the predominance of axial and transverse directions observed within buckling folds is compatible with a syn-folding origin of these fractures. Thus, transverse fractures develop parallel to the shortening direction, and axial fractures result from local extensional regimes due to curvature. However, it is always possible that the extension veins of the Essakane deposit were reactivated at the end of D1 during a decompression phase and/or during the second horizontal and perpendicular compression phase (D2) to D1. These veins suggest syn-

and post-deformation (D1) mineralization.

6. Conclusion

The Essakane deposit and its associated exploration projects in the far northeast of Burkina Faso were the subjects of a detailed petrographic and structural study to gain a better understanding of the structural control of mineralisation and gold timing. This study has identified three tectonic phases affecting the volcanic, sedimentary, and volcanosedimentary units of the Essakane region. They consist of: 1) horizontal shortening (D1) NE-SW, leading to the formation of P1 folds, axial plane schistosity S1, tension veins, and laminated (sheared) veins observed within the folded turbidites; 2) a second shortening phase (D2), characterised by a main stress (σ1) in an NW-SE direction, resulting in the formation of folds P2, planes S2-C and the boudinage of pre- and syn-D2 quartz veins; 3) a third N-S compression phase (D3), forming microfolds P3 and spaced cleavage S3. The structural analysis of gold mineralisation suggests that this is a case of epithermal to mesothermal gold deposits, with mineralisation hosted by stockwerks and hydrothermal breccias highlighting the deformation corridors in the zone. These veins are also observed within faulted folds (mainly (P1) on a hectometric scale). The veins observed in the Essakane deposit have directions that correspond to the structural patterns typical of an asymmetrical west-verging fold. Most of these veins appear to have formed during the first phase of deformation, which suggests that this phase is the possible maximum age of mineralisation.

Conflicts of Interest

The authors declare no conflicts of interest regarding the publication of this paper.

References

[1] Markwitz, V., Hein, K.A.A., Jessell, M.W. and Miller, J. (2016) Metallogenic Portfolio of the West Africa Craton. *Ore Geology Reviews*, **78**, 558-563. https://doi.org/10.1016/j.oregeorev.2015.10.024

[2] Goldfarb, R.J., André-Mayer, A., Jowitt, S.M. and Mudd, G.M. (2017) West Africa: The World's Premier Paleoproterozoic Gold Province. *Economic Geology*, **112**, 123-143. https://doi.org/10.2113/econgeo.112.1.123

[3] Milesi, J.-P., *et al.* (1989) Les minéralisations aurifères de l'Afrique de l'Ouest: Leurs relations avec l'évolution lithos-tructurale au Protérozoïque inférieur, No. 497. Editions BRGM, 3-98.

[4] Milési, J.P., Ledru, P., Ankrah, P., Johan, V., Marcoux, E. and Vinchon, C. (1991) The Metallogenic Relationship between Birimian and Tarkwaian Gold Deposits in Ghana. *Mineralium Deposita*, **26**, 228-238. https://doi.org/10.1007/bf00209263

[5] Fontaine, A., Eglinger, A., Ada, K., André-Mayer, A., Reisberg, L., Siebenaller, L., *et al.* (2017) Geology of the World-Class Kiaka Polyphase Gold Deposit, West African Craton, Burkina Faso. *Journal of African Earth Sciences*, **126**, 96-122. https://doi.org/10.1016/j.jafrearsci.2016.11.017

[6] Thébaud, N., Allibone, A., Masurel, Q., Eglinger, A., Davis, J., André-Mayer, A., *et al.* (2020) Chapter 34. The Paleoproterozoic (Rhyacian) Gold Deposits of West Africa.

In: Sillitoe, R.H., Goldfarb, R.J., Robert, F. and Simmons, S.F., Eds., *Geology of the World's Major Gold Deposits and Provinces*, Society of Economic Geologists, 735-752. https://doi.org/10.5382/sp.23.34

[7] Masurel, Q., Morley, P., Thébaud, N. and McFarlane, H. (2021) Gold Deposits of the ~15-Moz Ahafo South Camp, Sefwi Granite-Greenstone Belt, Ghana: Insights into the Anatomy of an Orogenic Gold Plumbing System. *Economic Geology*, **116**, 1329-1353. https://doi.org/10.5382/econgeo.4829

[8] Milési, J., Ledru, P., Feybesse, J., Dommanget, A. and Marcoux, E. (1992) Early Proterozoic Ore Deposits and Tectonics of the Birimian Orogenic Belt, West Africa. *Precambrian Research*, **58**, 305-344. https://doi.org/10.1016/0301-9268(92)90123-6

[9] Chardon, D., Bamba, O. and Traoré, K. (2020) Eburnean Deformation Pattern of Burkina Faso and the Tectonic Significance of Shear Zones in the West African Craton. *BSGF: Earth Sciences Bulletin*, **191**, Article No. 2. https://doi.org/10.1051/bsgf/2020001

[10] Groves, D.I., Goldfarb, R.J., Gebre-Mariam, M., Hagemann, S.G. and Robert, F. (1998) Orogenic Gold Deposits: A Proposed Classification in the Context of Their Crustal Distribution and Relationship to Other Gold Deposit Types. *Ore Geology Reviews*, **13**, 7-27. https://doi.org/10.1016/s0169-1368(97)00012-7

[11] Weinberg, R.F., Hodkiewicz, P.F. and Groves, D.I. (2004) What Controls Gold Distribution in Archean Terranes? *Geology*, **32**, 545-548. https://doi.org/10.1130/g20475.1

[12] Goldfarb, R.J., Baker, T., Dubé, B., Groves, D.I., Hart, C.J.R. and Gosselin, P. (2005) Distribution, Character, and Genesis of Gold Deposits in Metamorphic Terran. In: Hedenquist, J.W., Thompson, J.F.H., Goldfarb, R.J. and Richards, J.P., Eds., *One Hundredth Anniversary Volume*, Society of Economic Geologists, 407-450. https://doi.org/10.5382/av100.14

[13] Baratoux, L., Metelka, V., Naba, S., Jessell, M.W., Grégoire, M. and Ganne, J. (2011) Juvenile Paleoproterozoic Crust Evolution during the Eburnean Orogeny (~2.2 - 2.0 Ga), Western Burkina Faso. *Precambrian Research*, **191**, 18-45. https://doi.org/10.1016/j.precamres.2011.08.010

[14] Béziat, D., Siebenaller, L., Salvi, S. and Chevalier, P. (2016) A Weathered Skarn-Type Mineralization in Ivory Coast: The Ity Gold Deposit. *Ore Geology Reviews*, **78**, 724-730. https://doi.org/10.1016/j.oregeorev.2015.07.011

[15] Block, S., Ganne, J., Baratoux, L., Zeh, A., Parra-Avila, L.A., Jessell, M., *et al.* (2015) Petrological and Geochronological Constraints on Lower Crust Exhumation during Paleoproterozoic (Eburnean) Orogeny, NW Ghana, West African Craton. *Journal of Metamorphic Geology*, **33**, 463-494. https://doi.org/10.1111/jmg.12129

[16] Salvi, S., Amponsah, P.O., Siebenaller, L., Béziat, D., Baratoux, L. and Jessell, M. (2016) Shear-Related Gold Mineralization in Northwest Ghana: The Julie Deposit. *Ore Geology Reviews*, **78**, 712-717. https://doi.org/10.1016/j.oregeorev.2015.08.008

[17] Salvi, S., Sangaré, A., Driouch, Y., Siebenaller, L., Béziat, D., Debat, P., *et al.* (2016) The Kalana Vein-Hosted Gold Deposit, Southern Mali. *Ore Geology Reviews*, **78**, 599-605. https://doi.org/10.1016/j.oregeorev.2015.10.011

[18] Ducellier, J. (1963) Contribution à l'étude des formations cristallines et métamorphiques du Centre et du Nord de la Haute-Volta. Editions Technip.

[19] Delfour, J. and Jeambrun, M. (1970) Notice explicative de la carte géologique à 1/200000 (Oudalan). BRGM pour la D.G.M. de la République de Haute-Volta, Notice Explicative de Carte.

[20] Nikiema, S. (1992) Contexte structural et implications métallogénique au sein du permis

Essakane dans le sillon de Dori. CEMOB-BRGM.

[21] Tshibubudze, A. and Hein, K.A.A. (2016) Gold Mineralisation in the Essakane Goldfield in Burkina Faso, West African Craton. *Ore Geology Reviews*, **78**, 652-659. https://doi.org/10.1016/j.oregeorev.2015.10.030

[22] Peters, L. (2011) The Geology of East Markoye, Northeast Burkina Faso. Honours Thesis, University of the Witwatersrand. (Unpublished)

[23] Tshibubudze, A. and Hein, K.A.A. (2013) Structural Setting of Gold Deposits in the Oudalan-Gorouol Volcano-Sedimentary Belt East of the Markoye Shear Zone, West African Craton. *Journal of African Earth Sciences*, **80**, 31-47. https://doi.org/10.1016/j.jafrearsci.2012.11.010

[24] Castaing, C., *et al.* (2003) Notice explicative de la Carte géologique du Burkina Faso à 1/200,000. Bureau de Recherches Géologiques et Minières.

[25] Tshibubudze, A., Hein, K.A.A. and Marquis, P. (2009) The Markoye Shear Zone in NE Burkina Faso. *Journal of African Earth Sciences*, **55**, 245-256. https://doi.org/10.1016/j.jafrearsci.2009.04.009

[26] Kesse, G.O. (1985) The Mineral and Rock Resources of Ghana. A.A. Balkema Press.

[27] Bossière, G., Bonkoungou, I., Peucat, J. and Pupin, J. (1996) Origin and Age of Paleoproterozoic Conglomerates and Sandstones of the Tarkwaian Group in Burkina Faso, West Africa. *Precambrian Research*, **80**, 153-172. https://doi.org/10.1016/s0301-9268(96)00014-9

[28] Tunks, A.J., Selley, D., Rogers, J.R. and Brabham, G. (2004) Vein Mineralization at the Damang Gold Mine, Ghana: Controls on Mineralization. *Journal of Structural Geology*, **26**, 1257-1273. https://doi.org/10.1016/j.jsg.2003.11.005

[29] Koffi, Y.H., Djro, S.C. and Wenmenga, U. (2017) Lithostructural and Petrochemical Survey of Djarkadougou Gold Prospect (Southwest Burkina Faso/West Africa). *Earth Science Research*, **6**, 155-174. https://doi.org/10.5539/esr.v6n1p155

[30] Feybesse, J., Billa, M., Guerrot, C., Duguey, E., Lescuyer, J., Milesi, J., *et al.* (2006) The Paleoproterozoic Ghanaian Province: Geodynamic Model and Ore Controls, Including Regional Stress Modeling. *Precambrian Research*, **149**, 149-196. https://doi.org/10.1016/j.precamres.2006.06.003

[31] Hein, K.A.A. (2010) Succession of Structural Events in the Goren Greenstone Belt (Burkina Faso): Implications for West African Tectonics. *Journal of African Earth Sciences*, **56**, 83-94. https://doi.org/10.1016/j.jafrearsci.2009.06.002

[32] Hottin, G. and Ouédraogo, O.F. (1976) Carte géologique de la République de Haute-Volta. Direction de la Géologie et des Mines.

[33] Rogers, J.R. (2001) Technical Report: Essakane Project—Regional Mapping. Ranger Mineral NL, Rapport Interne.

[34] Fleuty, M.J. (1964) The Description of Folds. *Proceedings of the Geologists' Association*, **75**, 461-492. https://doi.org/10.1016/s0016-7878(64)80023-7

[35] de Kock, G.S., Armstrong, R.A., Siegfried, H.P. and Thomas, E. (2011) Geochronology of the Birim Supergroup of the West African Craton in the Wa-Bolé Region of West-Central Ghana: Implications for the Stratigraphic Framework. *Journal of African Earth Sciences*, **59**, 1-40. https://doi.org/10.1016/j.jafrearsci.2010.08.001

[36] Hein, K.A.A., Morel, V., Kagoné, O., Kiemde, F. and Mayes, K. (2004) Birimian Lithological Succession and Structural Evolution in the Goren Segment of the Boromogoren Greenstone Belt, Burkina Faso. *Journal of African Earth Sciences*, **39**, 1-23. https://doi.org/10.1016/j.jafrearsci.2004.05.003

[37] Tshibubudze, A., Hein, K.A.A. and McCuaig, T.C. (2015) The Relative and Absolute

Chronology of Strato-Tectonic Events in the Gorom-Gorom Granitoid Terrane and Oudalan-Gorouol Belt, Northeast Burkina Faso. *Journal of African Earth Sciences*, **112**, 382-418. https://doi.org/10.1016/j.jafrearsci.2015.04.008

[38] Beaudoin, G., Therrien, R. and Savard, C. (2006) 3D Numerical Modelling of Fluid Flow in the Val-D'or Orogenic Gold District: Major Crustal Shear Zones Drain Fluids from Overpressured Vein Fields. *Mineralium Deposita*, **41**, 82-98. https://doi.org/10.1007/s00126-005-0043-5

[39] Fitches, W.R., Cave, R., Craig, J. and Maltman, A.J. (1986) Early Veins as Evidence of Detachment in the Lower Palaeozoic Rocks of the Welsh Basin. *Journal of Structural Geology*, **8**, 607-620. https://doi.org/10.1016/0191-8141(86)90067-2

[40] Mawer, C.K. (1987) Mechanics of Formation of Gold-Bearing Quartz Veins, Nova Scotia, Canada. *Tectonophysics*, **135**, 99-119. https://doi.org/10.1016/0040-1951(87)90155-7

[41] Henderson, J.R., Wright, T.O. and Henderson, M.N. (1989) Mechanics of Formation of Gold-Bearing Quartz Veins, Nova Scotia, Canada—Comment. *Tectonophysics*, **166**, 351-352. https://doi.org/10.1016/0040-1951(89)90286-2

[42] Henderson, J.R., Henderson, M.N. and Wright, T.O. (1990) Water-Sill Hypothesis for the Origin of Certain Veins in the Meguma Group, Nova Scotia, Canada. *Geology*, **18**, 654-657. https://doi.org/10.1130/0091-7613(1990)018<0654:wshfto>2.3.co;2

[43] Jessell, M.W., Willman, C.E. and Gray, D.R. (1994) Bedding Parallel Veins and Their Relationship to Folding. *Journal of Structural Geology*, **16**, 753-767. https://doi.org/10.1016/0191-8141(94)90143-0

[44] Teixell, A., Durney, D.W. and Arboleya, M. (2000) Stress and Fluid Control on Décollement within Competent Limestone. *Journal of Structural Geology*, **22**, 349-371. https://doi.org/10.1016/s0191-8141(99)00159-5

[45] Sejourné, S. (2000) Étude structurale et géochimique des veines de l'écaille de Saint-Dominique, Appalaches du Sud du Québec. Master's Thesis, Université du Québec INRS Géoressources.

[46] Fyson, W.K. (1987) A Succession of Quartz Veins in Archean Metaturbidites, Yellowknife Bay, Slave Province. *Canadian Journal of Earth Sciences*, **24**, 698-710. https://doi.org/10.1139/e87-068

[47] Windh, J. (1995) Saddle Reef and Related Gold Mineralization, Hill End Gold Field, Australia; Evolution of an Auriferous Vein System during Progressive Deformation. *Economic Geology*, **90**, 1764-1775. https://doi.org/10.2113/gsecongeo.90.6.1764

[48] N.H.W. (1988) J.G. Ramsay & M.I. Huber 1987. *The Techniques of Modern Structural Geology*. *Volume* 2: *Folds and Fractures*. Xi + 391 pp. London, Orlando, San Diego, New York, Austin, Boston, Sydney, Tokyo, Toronto: Academic Press. Price UK £17.50 US $34.50 (Paperback). ISBN 0 12 576902 4 (Hard Covers); 0 12 576922 9 (Paperback). *Geological Magazine*, **125**, 316-317. https://doi.org/10.1017/s0016756800010384

[49] Geoff Tanner, P.W. (1989) The Flexural-Slip Mechanism. *Journal of Structural Geology*, **11**, 635-655. https://doi.org/10.1016/0191-8141(89)90001-1

[50] Geoff Tanner, P.W. (1990) The Flexural-Slip Mechanism: Reply. *Journal of Structural Geology*, **12**, 1085-1087. https://doi.org/10.1016/0191-8141(90)90107-a

[51] Cox, S.F., Sun, S.S., Etheridge, M.A., Wall, V.J. and Potter, T.F. (1995) Structural and Geochemical Controls on the Development of Turbidite-Hosted Gold Quartz Vein Deposits, Wattle Gully Mine, Central Victoria, Australia. *Economic Geology*, **90**, 1722-1746. https://doi.org/10.2113/gsecongeo.90.6.1722

[52] Kuenen, P.H. and de Sitter, L.U. (1938) Experimental Investigation into the Mechanism of Folding. *Leidse Geologische Mededelingen*, **10**, 217-239.

[53] Ramberg, H. (1964) Selective Buckling of Composite Layers with Contrasted Rheological Properties, a Theory for Simultaneous Formation of Several Orders of Folds. *Tectonophysics*, **1**, 307-341. https://doi.org/10.1016/0040-1951(64)90020-4

[54] Stearns, D.W. (1964) Macrofracture Patterns on Teton Anticline, Northwest Montana. *American Geophysical Union Transactions*, **45**, 107-108.

[55] McClay, K.R. (1987) The Mapping of Geological Structures, Geological Society of London Handbook. John Wiley & Sons.

[56] Bazalgette, L. (2004) Relations plissement/fracturation multi échelle dans les multicouches sédimentaires du domaine élastique/Fragile: Accommodation discontinue de la courbure par la fracturation de petite échelle et par les articulations. Possibles implications dynamiques dans les écoulements des reservoirs. Ph.D. Thesis, Université Montpellier II-Sciences et Techniques du Languedoc.